Biocatalysis and Agricultural Biotechnology 18 (2019) 101038

Contents lists available at ScienceDirect

Biocatalysis and Agricultural Biotechnology

journal homepage: www.elsevier.com/locate/bab

Surface functionalization of SBA-15 for immobilization of lipase and its application in synthesis of alkyl levulinates: Optimization and kinetics

Harshada M. Salvi, Ganapati D. Yadav*

Department of Chemical Engineering, Institute of Chemical Technology, Nathalal Parekh Marg, Matunga, Mumbai, 400019, India

ARTICLE INFO

Keywords:
Alkyl levulinates
Isoamyl alcohol
APTS
Lipase
Immobilization
Surface modification
Kinetics

ABSTRACT

Levulinic acid, being one the most important building block precursors, is of prime importance in a variety of industries. The esters of levulinic acid have significant applications in fields of flavor and fragrance. In this study, surface functionalized SBA-15 was used to immobilize *Candida antarctica* lipase B for the production of different alkyl levulinates. APTS (3-aminopropyl) triethoxysilane functionalized SBA-15 was used to immobilize lipase (Lip) cross-linked with GLU (glutaraldehyde) (named SBA-15-APTS-GLU-Lip). Various aspects of the immobilized catalyst were studied including surface area analysis, morphology, stability using XRD, SEM, TEM, and FTIR techniques. Process optimization of the model reaction of levulinic acid and isoamyl alcohol was done for the production of isoamyl levulinate. The highest conversion of 94% was achieved within 2 h at 50 °C. The kinetics was found to obey ternary dead end complex mechanism with isoamyl alcohol inhibition. The results indicate that the synthesized biocatalyst shows high operational stability and reusability up to 4 cycles.

1. Introduction

Biobased synthesis of value-added chemicals and biofuels is gaining high value. Levulinic acid (4-oxypentanoic acid) is considered as one of the top twelve chemicals which are derived from lignocellulosic biomass and is recognized as important specialty energy-rich chemicals because of its wide applications (dos Santos et al., 2013; Yadav and Yadav, 2014). The functional groups present in levulinic acid make it an ideal building block precursor for the synthesis of value-added chemicals such as levulinic esters, γ-valerolactone, and acrylic acid (Badgujar and Bhanage, 2016). Esters, particularly, are important derivatives for renewable fuel additives and precursors for polymer and resins production. They have huge applications in flavor and fragrance industry as well as blending components in biodiesel and biofuels (Nakhate and Yadav, 2016). Traditionally, these esters are synthesized by addition of homogeneous acid catalyst under high temperature which is not environment friendly. Enzymes being natural catalysts work under mild reaction conditions and are eco-friendly with low waste and lead to high selectivity (El-Nahass et al., 2018; Sheldon and van Pelt, 2013).

Lipase from the class of hydrolases has huge potential as biocatalyst due to its wide substrate array and its ability to carry out various transformations such as esterification, transesterification, aminolysis, acylation, and acetylation in non-aqueous media providing vast applications in large-scale industries. Furthermore, they are reasonably thermostable, highly enantioselective and stereospecific (Hu et al., 2012). *Candida antarctica* lipase B (CAL B) constitutes of 317 amino acids. It has a molecular mass of 37 kDa (Salvi et al., 2018). CAL B has been immensely used for esterification reactions due to its properties of good thermal stability and high selectivity towards the product.

Immobilization of enzymes is of prime significance. The immobilization of lipase not only facilitates easy separation of product and recovery but also confers advantages such as enhanced stability both thermodynamically and kinetically, improved activity, and selectivity (Bommarius and Paye, 2013; Holz et al., 2018). Reusability is one of the important advantages of immobilization which is of marked importance. Reusability enables reuse of enzyme which ultimately reduces the cost of enzyme and gives a more practical approach for industrial application (Sheldon and Woodley, 2018). Despite the existence of commercially available catalysts, various methods of immobilization have been developed by a number of researchers including physical adsorption, covalent binding, cross-linking, encapsulation, and entrapment (Li et al., 2018; Poojari and Clarson, 2013). Among these, physical adsorption and covalent binding are the most popular techniques. Although physical adsorption is the simplest and low-cost method of immobilization, the loss of enzyme is high due to weak interaction between enzyme and support which leads to leaching (Kamble et al., 2016). Further, covalent binding is the next possible option. The covalent binding involves a reaction between functional groups of the

---

* Corresponding author.
E-mail address: gd.yadav@ictmumbai.edu.in (G.D. Yadav).

https://doi.org/10.1016/j.bcab.2019.101038
Received 23 October 2018; Received in revised form 24 January 2019; Accepted 10 February 2019

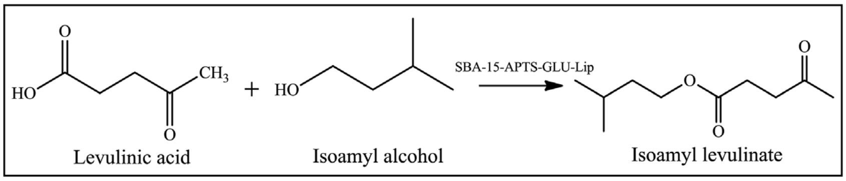

Scheme 1. Synthesis of isoamyl levulinate from levulinic acid and isoamyl alcohol.

support material and functional groups of enzyme which mainly include $-NH_2$, $-SH$ and $-OH$ (Zdarta et al., 2018b). The properties of immobilization can be tailored by changing the supports, techniques, conditions, and the addition of a linker or a binder (Cai et al., 2016; Zhou et al., 2018).

A wide variety of supports are available for immobilization of enzymes and classically divided into two groups as inorganic and organic materials. The inorganic materials are further classified into silica and inorganic oxides, minerals, and carbon-based materials. The organic materials include synthetic polymers and natural biopolymers. (Jesionowski et al., 2014; Zdarta et al., 2018a, 2018b). Inorganic supports, particularly silica-based materials, have good thermal, chemical and mechanical resistance, and are cheap and easily available with non-complicated synthesis procedure. The groups present on the surface of inorganic materials such as hydroxyl, carbonyl, and carboxyl enables easy functionalization which ultimately helps in higher stability and reusability (Zdarta et al., 2018c).

Mesoporous materials (2–50 nm) are one such class of inorganic materials which are ideal for immobilization of enzymes. The mesoporous supports can be easily tailored by adjusting the synthesis conditions for obtaining the desired pore structure. This property of mesoporous supports distinguishes it from other materials suitable for enzyme immobilization (Zdarta et al., 2018a). The M41S family of mesoporous materials was first reported in 1992 (dos Santos et al., 2013). Ever since MCM-41 and SBA-15 (Santa Barbara Amorphous) have been the most abundantly used mesoporous materials among all. SBA-15 prepared through the acid media was first reported by Zhao et al., in 1998 (Zhao et al., 1998). With the well-defined pore structure, good hydrothermal stability, inert framework, biocompatibility, and large surface area, SBA-15 is one of the extensively used materials (Gao et al., 2010; Kruk et al., 2000). SBA-15 has applications in various fields such as catalysis, immobilization, adsorption, and also for drug delivery systems (Bhange et al., 2014).

Silica-based supports are one of the natural and most promising supports for enzyme immobilization which have been extensively exploited. Yadav and Jadhav (2005) studied hexagonal mesoporous silica (HMS) as support for pre-immobilization of *Candida antarctica* lipase B (CAL B), *Pseudomonas cepacia* lipase (PSL), *Candida rugosa* lipase (CRL) and porcine pancreatic lipase (PPL) and the effect of calcium alginate encapsulation was covered. Hude et al. (2016) used *penicillium camembertii* lipase supported on glutaraldehyde activated-SBA-15 for mono-esterification of bioglycerol in non-aqueous media. Magadum and Yadav (2017, 2018) have used mesocellular foam (MCF) silica for supporting metal and lipase in achieving excellent selectivity in tandem or cascade engineered catalyzed reactions. Glucose oxidase was immobilized on magnetic silica with glutaraldehyde as linker wherein a good activity of 95% was achieved after immobilization (Jaquish et al., 2018). Hierarchical mesoporous silica called CBZ silica, synthesized from sodium silicate, was used for immobilization of *Thermomyces lanuginosus* lipase (Soto et al., 2017). In another study, immobilization of CAL B was achieved using silica-lignin hybrid matrix which exhibited 80% activity with increased thermal and chemical stability (Zdarta et al., 2016). SBA-15 is a popular support for immobilization of enzymes. The effect of pore diameter of SBA-15 on immobilization of CAL B was studied by using physical adsorption for diacylglycerols synthesis by Cai et al. (2016). González-Delgado et al. (2018) studied β-galactosidase immobilization on ultra-large pore SBA-15 using covalent glyoxyl immobilization method to get the best catalytic performance and productivity with efficient reutilization. Gao et al. (2010) reported immobilization of *Candida rugosa* on SBA-15 using glutaraldehyde as a cross-linker adsorbed with chitosan to make a mesh-like structure creating an extensive and stable network. Microwave assisted synthesis of SBA-15 was carried by Calavia (2014) for CO_2 capture to intensify the process hours from days. Immobilization of recombinant CAL B on SBA-15 was carried out for kinetic resolution of (R, S)- phenylethyl acetate (Rios et al., 2016).

Although immobilization of lipase with glutaraldehyde (GLU) has been immensely studied and critically evaluated in the past, the crosslinking method does not prove to be completely efficient. Thus, there is scope to improve the performance of immobilized lipases (Yadav and Jadhav, 2005) and the current work was so planned to examine the catalytic activities of CALB on SBA-15 through physical adsorption, crosslinking with glutaraldehyde and with covalent binding using (APTS) (3-aminopropyl) triethoxysilane. SBA-15 was surface functionalized with APTS and later cross-linked with glutaraldehyde to support CAL B. It was used to carry out reaction between levulinic acid and isoamyl alcohol to produce isoamyl levulinate (3-methyl butyl 4-oxopentanoate) (Scheme 1). The mechanistic and kinetic studies are also presented. The results prove that the catalyst is superior to the previously reported literature.

2. Materials and methods

2.1. Enzymes and chemicals

Candida antarctica lipase B (CAL B) was procured as a gift sample from Advanced Enzymes Ltd., India. Triblock copolymer P123 and (3-Aminopropyl) triethoxysilane were purchased from Alfa Aesar, Sigma Aldrich respectively. HCL, tetraethoxysilane, levulinic acid, isoamyl alcohol, and all solvents were used from S D Fine Chemicals Ltd, Mumbai, India.

2.2. Synthesis of support

The support SBA-15 was prepared according to the method given by Zhao et al. (1998) with slight modification. The surfactant triblock copolymer template used was pluronic 123. Pluronic 123 (4 g) was dissolved in 20 ml of 37 wt % HCl and 120 ml of distilled water. It was mixed and stirred for 3 h at 313 K. 9 ml of tetraethoxysilane was added and the final solution was stirred for 24 h. The temperature was further raised to 373 K and maintaned for 24 h without stirring. Post filtration and washing, the solid was dried at 373 K and then calcined at 823 K for 6 h.

2.3. Characterization of support

The synthesized SBA-15 support was well characterized by different techniques. Powder X-ray diffraction of calcined SBA-15 was performed using (Philips X'Pert System diffractometer using Cu Kα radiation, λ = 1.5418 Å). The surface area and pore volume were calculated using BET surface area analyzer (Micromeritics ASAP, 2010 instrument) with the nitrogen adsorption isotherm at −196 °C. FT-IR was carried out using Perkin- Elmer Spectrum BX spectrometer. Scanning electron microscopy (SEM) was conducted using a JEOL JSM 840 and transmission

Table 1
Enzyme activity of various methods of immobilization.

Immobilization	Activity (Units/g)
Free Lip	2520 ± 4.08
SBA-15-APTS-GLU-Lip	2100 ± 5.55
SBA-15-GLU-Lip	1800 ± 6.23
SBA-15-Lip	1111 ± 4.49

electron microscopy (TEM) using JEOL 2010.

2.4. Immobilization procedure

2.4.1. Surface functionalization of SBA-15 with APTS

For hydrolysis of support, 0.25 g of APTS was added to 200 g of 1 M aq HCl at room temperature. 1 g of the previously synthesized SBA-15 was added to it and shaken in a rotary shaker for 8 h at 160 rpm. The obtained suspension was kept at 100 °C for 24 h. The resulting powder was filtered and washed with deionized water and ethanol, then dried at 80 °C for 12 h.

2.4.2. Activation with glutaraldehyde cross-linking of lipase immobilized on SBA-15

The surface functionalized SBA-15 with APTS was pre-equilibrated for 2 h in 10 ml of phosphate buffer (100 mM, pH 7.5) in a shaker incubator at 180 rpm. Further, 0.1% (w/w) of glutaraldehyde solution was added and then incubated for 1 h at 180 rpm.

2.4.3. Immobilization of enzyme on modified SBA-15

One ml of crude liquid *Candida antarctica* lipase B was diluted with 10 ml of phosphate buffer solution. This diluted enzyme preparation was added to the above solution of surface functionalized SBA-15 with ATPS and glutaraldehyde. It was then vortexed for 30 s and sonicated for 10 s. The solution was kept for 1 h in a shaker incubator at 25 °C at 180 rpm. The supernatant was washed with buffer three times and then collected by centrifugation at 3578 × g at 4 °C for 20 min. The immobilized enzyme was then stored at 4 °C.

2.5. Enzyme activity and protein estimation

The activity of the immobilized enzyme was calculated using tributyrin assay (Charusheela and Arvind, 2002). A solution (250 µl) of the enzyme was added to 1062 µl of 0.1 M sodium phosphate buffer (pH 7). To the above mixture, 188 µl tributyrin was added. This mixture was vortexed for 15 min at 30 °C. The reaction was terminated by adding 10 ml of methanol and immediately titrated against 0.05 M NaOH solution using phenolphthalein as indicator. The protein content was determined according to the procedure given by Bradford (1976). The calibration curve was plotted using bovine serum albumin (BSA) as a standard protein. 100 µl of sample was added to 5 ml of Bradford reagent and incubated for 5 min. The absorbance was measured at 595 nm.

The activity of each sample was calculated as follows:

Sample activity (TBU, tributyrin unit) = (ml titrant × molarity of titrant × 1000 × dilution factor)/(time × volume of enzyme)

1 TBU is the quantity of enzyme which releases 1 µmol titratable butyric acid per min under the assay conditions.

2.6. Experimental setup

All experiments were carried out in a typical 50 cm^3 capacity batch reactor with 3 cm i.d. and four baffles. The agitator was equipped with six blades pitched turbine impeller. The reaction consisted of 0.01 mol of levulinic acid, 0.02 mol of isoamyl alcohol, methyl tert-butyl ether as solvent up to 15 ml of volume, temperature 50 °C, 50 mg of enzyme loading and 400 rpm agitation. The analysis of the reaction was done using gas chromatography (GC) (Thermo Scientific Trace 1110), equipped with FID and TG5MS capillary column. The initial temperature was set at 70 °C. It was raised at a ramp rate of 17 °C/min up to 250 °C with a hold time of 2 min. The nitrogen flow was maintained at 1 ml/min. The injector and detector temperature were maintained at 280 °C. The product confirmation was done using GC-MS (Thermo Scientific Trace 1300 ISQ LT) (see Supplementary Information (SI), Fig. S1).

2.7. Lineweaver-Burk plot

The enzyme kinetics study was carried out to investigate the impact of different substrate concentrations on the rate of reaction. For the determination of the kinetic model, the reactant and substrate concentrations were studied over a wide range. In one set of the experiment, the concentration of levulinic acid was varied from 0.01 mol to 0.04 mol by keeping the concentration of isoamyl alcohol constant. In another set of experiment, the concentration of isoamyl alcohol was varied from 0.01 to 0.04 mol by keeping levulinic acid constant. In both the cases, the total reaction volume was kept constant. The Lineweaver-Burk plot of reciprocal of initial rate versus reciprocal of the concentration of substrate was made on the basis of initial rates.

3. Results and discussion

3.1. Immobilization of lipase on SBA-15

Table 1 shows the comparison of activities of lipase supported on SBA-15 with free lipase, physical adsorption (SBA-15-lip), cross-linked lipase (SBA-15-GLU-lip) and surface functionalized and cross-linked (SBA-15-APTS-GLU-Lip). The activity of free lipase calculated using tributyrin assay was 2520 ± 4.08 Units/g and that of SBA-15-APTS-GLU-Lip was 2100 ± 5.55. It can be observed that the highest activity is seen with SBA-15-APTS-GLU-Lip among the immobilized enzymes. The aminosilane APTS has high aqueous stability and a highly reactive amino group which acts as a primer to form a bridge, helping in strong bondage (Bauer et al., 2017). Unlike in others SBA-15-GLU-Lip, SBA-15-Lip, the leaching of the enzyme could take place. The forces that act between support and enzyme include van der Waals forces and hydrogen bonding and hydrophobic interactions (Hude et al., 2016). Later after surface functionalization, covalent bonding takes place between the modified support and enzyme. Covalent immobilization provides high immobilized stability and makes certain the highest strength between support and enzyme, minimizing the leakage issues (Guzik et al., 2014). Hence, the highest activity was retained in SBA-15-APTS-GLU-Lip.

3.2. Characterization of support SBA-15

3.2.1. BET

The textural properties of the support obtained from N_2 adsorption have been mentioned in Table 2. The surface area characterization helps to confirm that the enzyme has been adsorbed on the support. The

Table 2
Textural properties of the support from N_2 adsorption.

Material	Surface area (m^2/g)	Pore volume (cm^3/g)	Pore size (nm)
SBA-15	406.5	1.24	5.8
SBA-15-APTS	317.7	0.35	7.6
SBA-15-APTS-GLU-Lip	254.2	0.32	8.3
Reused (1 cycle) SBA-15-APTS-GLU-Lip	240.7	0.27	8.1

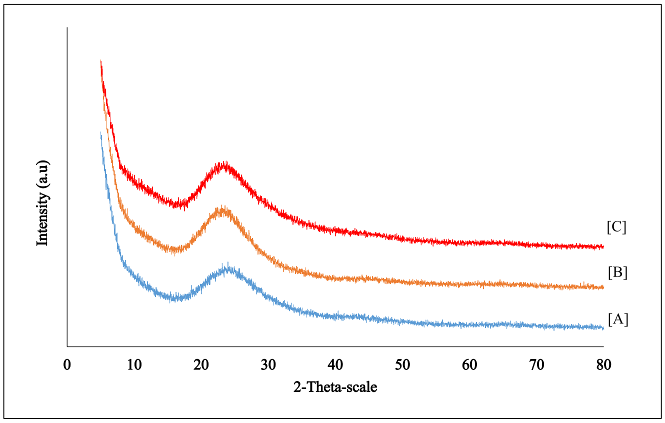

Fig. 1. XRD patterns of [A] SBA-15, [B] SBA-15-APTS and [C] SBA-15-APTS-GLU-Lip.

surface area of SBA-15 was obtained to be 406.5 m^2/g and that with SBA-15-APTS and SBA-15-APTS-GLU-Lip were 317.7 and 254.2 m^2/g, respectively. As expected due to surface functionalization of APTS on SBA-15 and further with lipase, the surface area is decreased. It could be observed that the pore volume remained almost constant. This can be due to blocking of small pores due to binding of APTS, glutaraldehyde, and enzyme (Nguyen et al., 2008).

3.2.2. XRD

Fig. 1compares the XRD patterns of [A] SBA-15, [B] SBA-15-APTS and [C] SBA-15-APTS-GLU-Lip. The pattern shows a similarity between all the three materials (Parent material, surface functionalized material and one after immobilization). The similarity indicates that the functionalization of APTS and lipase does not affect significantly order of the structure (Doadrio et al., 2014). There is a single peak which can be observed in the range of $2\theta = \sim 24^\circ$ in all the three samples. The absence of a sharp peak indicates the amorphous nature of the material (Chong and Zhao, 2003) and the full-width half maximum of $\sim 6^\circ$ shows the high degree of amorphous nature. The low angle XRD measurements for SBA-15 were obtained for 2θ range from 2° to 10°. As the literature shows the main characteristic peaks of two-dimensional hexagonal pore arrangement materials such as SBA-15 refer to the crystal planes corresponding to Miller indices of 100, 110 and 200 which fall in 2 θ range of 0.6°–2° (Cai et al., 2016; dos Santos et al., 2013). The instrument had limitations and hence peaks in the 2θ range of 0.5–2 are not seen in our case (SI, Fig. S2).Hence FTIR and BET were also used.

3.2.3. FTIR

Fig. 2 shows the FT-IR spectra of SBA-15 before and after modification, namely, [A], [B] and [C]. In the IR spectra of SBA-15 before modification, the peaks at 3454 cm^{-1} and 1086 cm^{-1} (asymmetric stretching) belong to silanol groups (He et al., 2006). Also, the broad envelope band at 3454 cm^{-1} is due to physisorbed water and surface hydroxyls which can be observed in all samples before and after modification of SBA-15. The peak at 1636 cm^{-1} is represented by the bending vibrations of physically adsorbed water molecules (Dai et al., 2017). It is difficult to identify the functional group of $-NH_2$ attached on the surface of modified SBA-15 as these peaks are overlapped with the O−H vibrations. The peak at 2854 cm^{-1} and 2926 cm^{-1} weak bands are due to stretching vibrations of the C−H moiety. Typical Si−O−Si bands 1086 and 800 cm^{-1} are attributed to the condensed silica framework of SBA-15. Trough associated bending of Si−OH bonds is in the range of 965 cm^{-1} (Hude et al., 2016). It can be observed that there is a decrease in the intensity of the silanol group after enzyme immobilization and surface functionalization due to weakened surface hydroxyl groups which are reduced after the surface modification of SBA-15 (Zou et al., 2014).

3.2.4. SEM

Large parallel rod-like structures of 1–5 µm in length were observed in Fig. 3 which was very similar to the one reported by Hude et al. (2016). They consist of agglomerated long fibers. The image [B] shows that the morphology of SBA-15 remains the same even after surface functionalization. The immobilization of lipase on SBA-15 can be clearly seen in the image [C]. Also, the SEM of reused catalyst which was recovered after one reaction is shown in the image [D]. It confirms that the structure of the parent material SBA-15 remains intact after the reaction as well.

3.2.5. TEM

The TEM images of pure SBA-15 and functionalized SBA-15-APTS-GLU-Lip are compared in Fig. 4. The TEM investigations show well ordered long-range one-dimensional mesoporous channels in both the images. The pores of the rod-like particles run parallel to the long axis of the rod. Thus it can also be proved that the morphology has been maintained after functionalization and immobilization procedure. A similar result is reported by Hude et al. (2016). Also, the resulting material is an amorphous phase which is in good agreement with XRD results. The overlapping in the image [B] clearly shows the immobilization of lipase on the parent material.

4. Optimization studies

The optimization studies were carried out for the reaction between levulinic acid and isoamyl alcohol using the catalyst SBA-15-APTS-GLU-Lip for the production of isoamyl levulinate as shown in Scheme 1.

4.1. Effect of solvent

The solvent study was carried out using various solvents based on the solubility of levulinic acid. The study was carried out using solvents based on the *logP* value as solvents play a crucial role in the performance of enzyme activity. In this study methyl tert-butyl ether (MTBE), tetrahydrofuran (THF) and 1, 4 dioxane were used as shown in Fig. 5. MTBE showed maximum conversion which was then followed by THF and 1, 4 dioxane. Usually, hydrophobic solvents are preferred as they do not distort the essential water layer required by the lipase for its activity (Salvi et al., 2018). Thus MTBE was selected further as it gave a maximum conversion of 78% of isoamyl levulinate.

4.2. Effect of speed of agitation

The effect of speed of agitation is an important parameter to study external mass transfer resistance. The study was carried out in the range of 200–500 rpm (Fig. 6). With the increase in speed of agitation, increase in conversion of isoamyl levulinate was observed. The maximum conversion of 75% was achieved at 300 rpm. However, the conversion was decreased with an increase in speed of agitation at 400 and 500 rpm. This may be due to the reduction in number of particles in the liquid phase at higher speed since the particles are thrown out and stick on the wall surface of the reactor (Yadav and Trivedi, 2003). Hence, optimum speed of agitation of 300 rpm was selected for further study.

4.3. Effect of catalyst loading

The effect of catalyst loading was studied in the range of 20–200 mg (Fig. 7). It was found that the initial rate of reaction increased with increased loading of immobilized enzyme. After loading of 150 mg, there was no significant increase in the conversion at 200 mg. So it can be concluded that the amount of catalytic sites was higher than that required for the reaction. The maximum conversion of 83% was achieved at a catalyst loading of 150 mg in 2 h. This catalyst loading

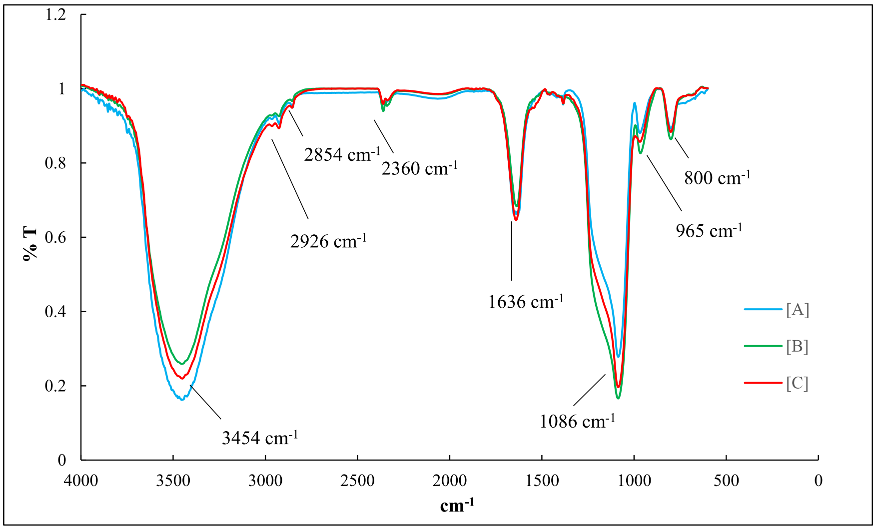

Fig. 2. FT-IR spectra of [A] SBA-15, [B] SBA-15-APTS and [C] SBA-15-APTS-GLU-Lip.

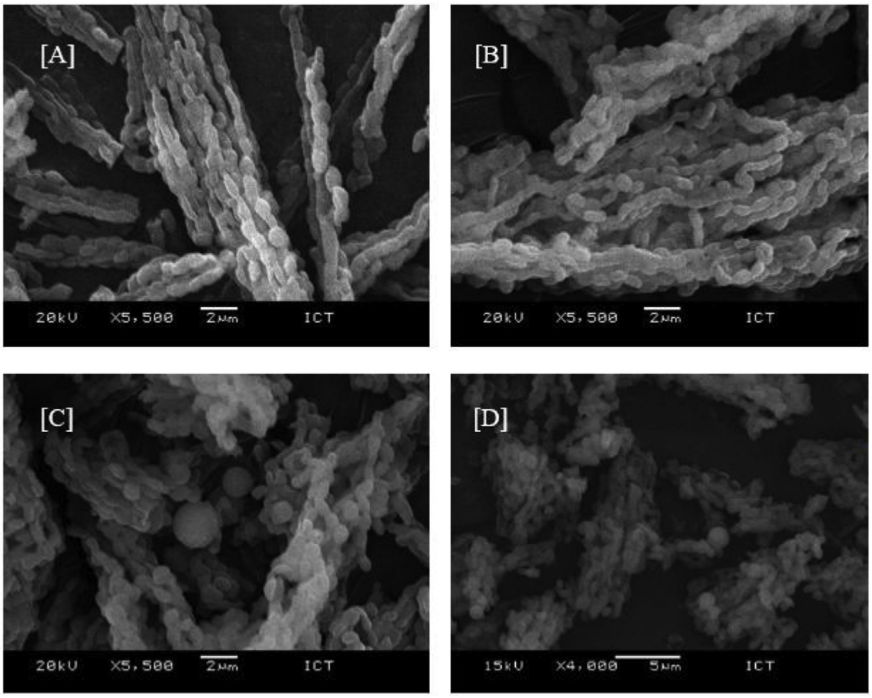

Fig. 3. SEM images of [A] SBA-15, [B] SBA-15-APTS, [C] SBA-15-APTS-GLU-Lip and [D] reused SBA-15-APTS-GLU-Lip.

was used for further reactions.

4.4. *Effect of temperature*

The effect of temperature was studied in the range of 30–60 °C (Fig. 8). It was clearly observed that the conversion increased with increase in temperature and also that the reaction is temperature dependent which can be observed with high initial conversions. There was not much difference in the conversion at 50 °C and 60 °C. Thus 50 °C was considered as an optimum temperature. The activation energy for the reaction was calculated to be 4.19 kcal/mol from the Arrhenius plot (SI Fig. S3). The general activation energy range for enzymatic reaction is below 6 kcal/mol (Yadav and Borkar, 2008). So the calculated activation energy falls in the general range.

4.5. *Effect of mole ratio*

The mole ratio study was carried out by varying the concentration of both levulinic acid and isoamyl alcohol. Four different ratios of levulinic acid and isoamyl alcohol 1:1, 1:2, 1:3, and 1:4 were studied (Fig. 9). With the increase in the concentration of isoamyl alcohol, conversion decreased. This is due to the inhibitory effect of isoamyl alcohol. Maximum conversion of 94% was obtained with 1: 2 mol ratio of levulinic acid to isoamyl alcohol. Also, isoamyl alcohol has an inhibitory effect as it has a low *logP* value of 1.3, and it strips of the essential water layer surrounded by the enzyme and decreases its activity. Further, the long chain of isoamyl alcohol destabilizes the native conformation of lipase due to the hydrophobic-hydrophobic interaction between lipase and isoamyl alcohol (Badgujar and Bhanage, 2014; Bhavsar and Yadav, 2018). This is further discussed in Section 4.8 on enzyme kinetics.

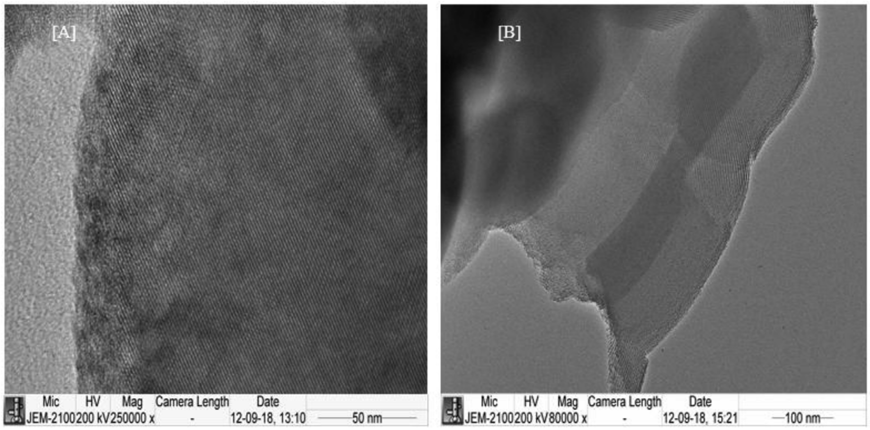

Fig. 4. TEM images of [A] SBA-15, [B] SBA-15-APTS-GLU-Lip.

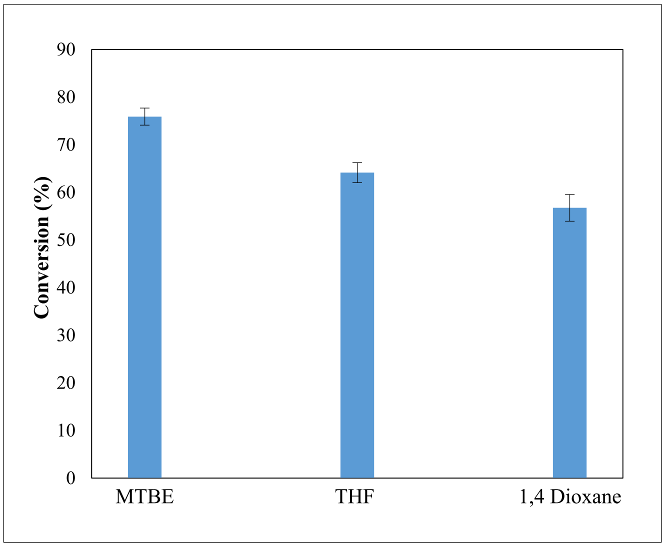

Fig. 5. Effect of various solvents (Reaction conditions: levulinic acid 0.01 mol, isoamyl alcohol 0.02 mol, temp 40 °C, catalyst loading 100 mg, solvent up to 15 ml).

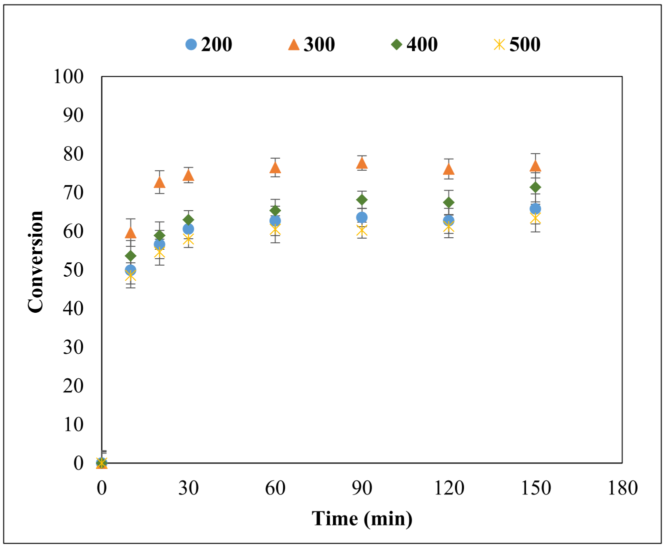

Fig. 6. Effect of speed of agitation (Reaction conditions: levulinic acid 0.01 mol, isoamyl alcohol 0.02 mol, temp 40 °C, catalyst loading 100 mg, solvent up to 15 ml).

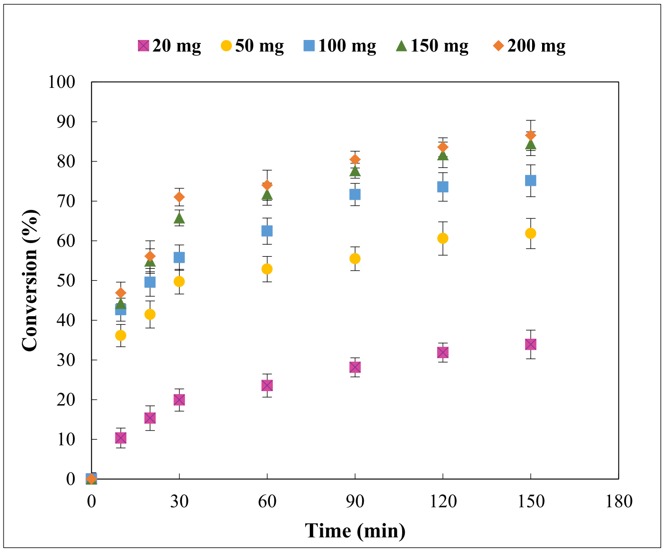

Fig. 7. Effect of catalyst loading (Reaction conditions: levulinic acid 0.01 mol, isoamyl alcohol 0.02 mol, temp 40 °C, speed of agitation 300 rpm, solvent methyl tert-butyl ether up to 15 ml).

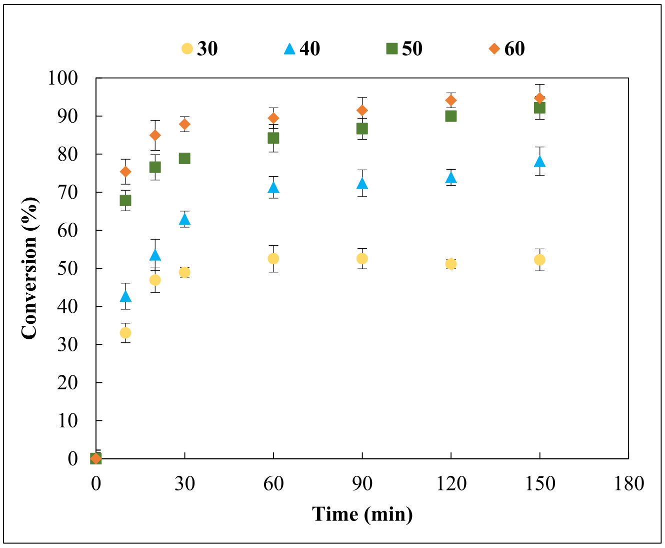

Fig. 8. Effect of temperature (Reaction conditions: levulinic acid 0.01 mol, isoamyl alcohol 0.02 mol, speed of agitation 300 rpm, catalyst loading 150 mg, solvent methyl tert-butyl ether up to 15 ml).

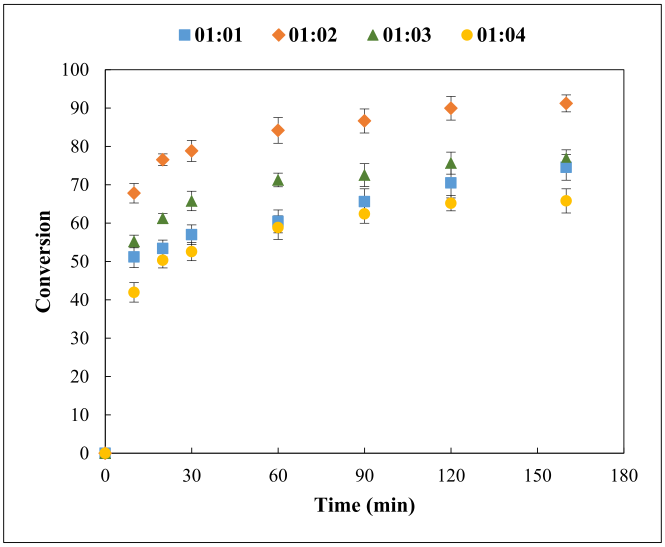

Fig. 9. Effect of mole ratio (Reaction conditions: speed of agitation 300 rpm, catalyst loading 150 mg, temp 50 °C, solvent methyl tert-butyl ether up to 15 ml).

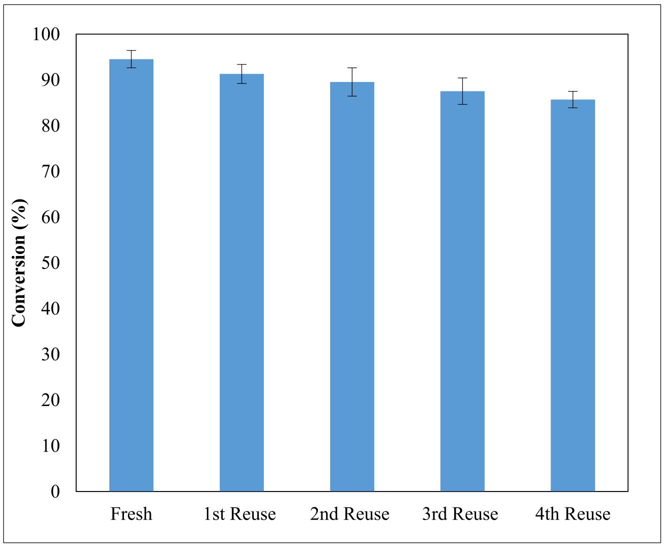

Fig. 10. Reusability (Reaction conditions: levulinic acid 0.01 mol, isoamyl alcohol 0.02 mol, speed of agitation 300 rpm, catalyst loading 150 mg, temp 50 °C, solvent methyl tert-butyl ether up to 15 ml).

4.6. Effect of acyl donors

Since the model reaction of levulinic acid esterification with isoamyl alcohol gave a higher conversion of 94% isoamyl levulinate, we extended the study to evaluate the effect of varying acyl donor chain length. Previously, similar work was carried out in our group using a chemical catalyst UDCaT-5, a mesoporous super acidic zirconia modified catalyst. Various acyl donors were studied from methanol to benzyl alcohol which showed conversions in the range of 90–100% (Yadav and Yadav, 2014). Similarly, under the optimized conditions, various acyl donors were applied for the synthesis of levulinate esters using the catalyst SBA-15-APTS-GLU-Lip. In the present study, we have synthesized seven levulinate compounds as given in Table 3. All the products were confirmed using GCMS (SI Fig. S4–S9). It can be observed that conversion increased with an increase in chain length of the acyl donor. The maximum conversion of 94% was obtained for isoamyl levulinate and the lowest of 71% was obtained for methyl levulinate. It is well known that the alcohols such as methanol and propanol have an inhibitory effect on lipase reducing its activity. Thus, a lower conversion was obtained with methyl levulinate and ethyl levulinate due to high polarity of alcohols leading to inactivation of the enzyme (Zhou et al., 2018).

Table 3
Synthesis of various levulinic acid esters using SBA-15-APTS-GLU-Lip.

No.	Levulinate esters	Name	Conversion (%)
1	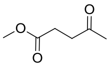	Methyl levulinate	71
2	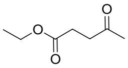	Ethyl levulinate	73
3	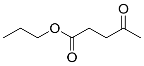	Propyl levulinate	76
4	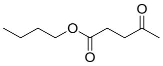	Butyl levulinate	85
5	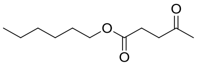	Hexyl levulinate	90
6	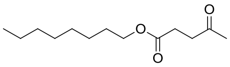	Octyl levulinate	92
7	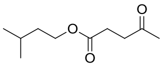	Isoamyl levulinate	94

(Reaction conditions: levulinic acid 0.01 mol, acyl donor 0.02 mol, speed of agitation 300 rpm, catalyst loading 150 mg, temp 50 °C, solvent methyl tert-butyl ether up to 15 ml).

4.7. Reusability study

The reusability study is of prime importance because it determines the enzyme stability and greatly influences its cost in industrial operation. The immobilized enzymes can be easily separated from the reaction mixture and reused increasing the overall biocatalytic productivity. The catalyst was recovered after each experiment by filtration, washed with methyl tert-butyl ether, dried for 12 h at room temperature and reused. The biocatalyst showed better reusability and was found to be stable for reuse up to 4 cycles. A decrease in conversion of isoamyl levulinate could be observed in Fig. 10. There is no makeup catalyst added. The decrease in the conversion of isoamyl levulinate with each cycle is due to loss of catalyst during filtration and use (~5%) and loss of enzyme activity due to leaching of the enzyme from the support. The residual activity of the immobilized enzyme retained after the 4th cycle was found out to be 2011 ± 3.39 Units/g. The other reason for the decrease in conversion is due to enzyme inhibition due to isoamyl alcohol which was confirmed in Section 4.8 on *Enzyme kinetics*.

4.8. Enzyme kinetics

The enzyme kinetics was studied to analyze the reaction mechanism. The Lineweaver-Burk plot of reciprocal of initial rate versus reciprocal of the concentration of levulinic acid (so called double inversion) is illustrated in Fig. 11. Since the lines are intersecting at a certain point, it can be concluded that the reaction follows ternary dead end complex with inhibition by isoamyl alcohol.

The ternary complex mechanism can be depicted in Cleland's notation, as follows.

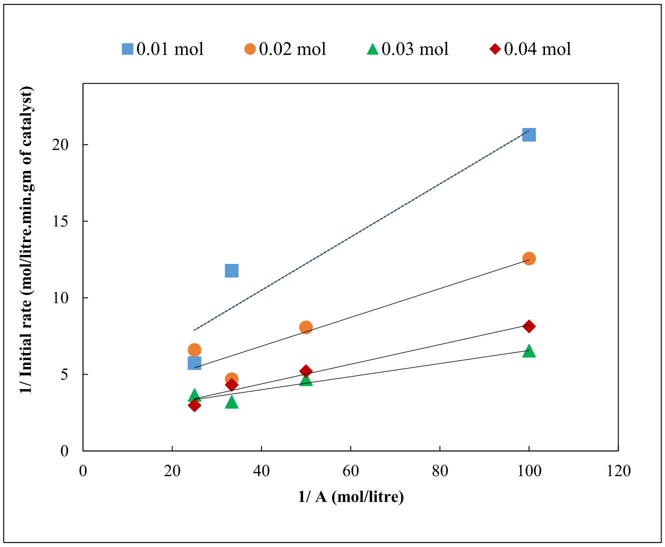

Fig. 11. Lineweaver-Burk plot of 1/initial rate Vs 1/[A] at different concentrations of B.

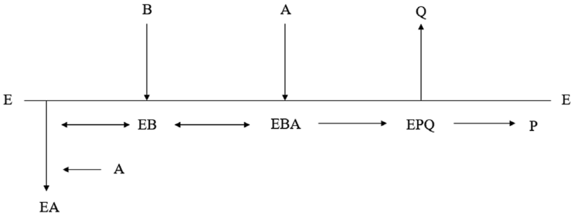

Where.

E − Enzyme
A - Levulinic acid
B - Isoamyl alcohol
P - Isoamyl levulinate
Q - Water
EA - Enzyme acyl complex
EAB - Ternary complex with enzyme and reactants A, B
EPQ - Ternary complex with enzyme, isoamyl levulinate and water

The rate equation for the above model can be given as

$$v = \frac{v_{\max}[A][B]}{K_{mB}[A] + K_{mA}[B]\left(1 + \frac{[B]}{K_{iB}}\right) + [A][B]}$$

Where.

[A]- Concentration of Levulinic acid (mol L^{-1})
[B]- Concentration of isoamyl alcohol (mol L^{-1})
K_{mA} - Michaelis constant (mol L^{-1})
K_{mB} - Michaelis constant for isoamyl alcohol (mol L^{-1})
K_{iB} - Inhibition constant of isoamyl alcohol (mol L^{-1})
V- Initial rate of reaction (mol L^{-1} $\min^{-1}$)
$V_{\max}$ - Maximum rate of reaction (mol L^{-1} $\min^{-1}$)

Kinetic constants were calculated by using Polymath 6.0 software. The values are as follows $V_{\max} = 0.28$ mol L^{-1} $\min^{-1}$, $K_{mA} = 0.629$ mol L^{-1}, $K_{mB} = 0.015$ mol L^{-1}, $K_{iB} = 0.021$ mol L^{-1}. Also the parity plot of calculated rates and experimental dates was plotted which confirms the validity of the model (R^2 0.96) (SI Fig. S10)

5. Conclusion

Synthesis of various alkyl levulinates using newly fabricated SBA-15-APTS-GLU-Lip was successfully performed. *Candida antarctica* lipase B was immobilized on surface functionalized SBA-15 using APTS and cross-linked with glutaraldehyde. The results indicated that SBA-15-APTS-GLU-Lip showed higher activity than only cross-linked SBA-15-GLU-Lip. In the model reaction of isoamyl levulinate synthesis, 94% conversion was achieved at optimum conditions of 1:2 mol ratio of levulinic acid: isoamyl alcohol, 300 rpm, and 50 °C in 2 h. Also, the scope of the reaction was studied by using different acyl donors which can be further extended for the organic synthesis of various chemicals. The kinetics was found to obey ternary dead-end complex mechanism with isoamyl alcohol inhibition. The catalyst was reused up to 4 cycles, and from the results, it can be concluded that it has good stability. The above results imply that SBA-15-APTS-GLU-Lip is a promising catalyst. It helps us in understanding the surface modification which is more favorable for enzyme attachment which ultimately increases its reusability which may help in the development of stable biocatalyst for future applications in different areas.

Acknowledgment

HMS acknowledges University grants commission for the award of SRF and providing fellowship through UGC-BSR programme. GDY acknowledges the financial support from R.T. Mody Distinguished Professor Endowment, Tata Chemicals Darbari Seth Distinguished Professor of Leadership and Innovation, and J. C. Bose National Fellowship by Department of Science & Technology- Government of India.

Appendix A. Supplementary data

Supplementary data to this article can be found online at https://doi.org/10.1016/j.bcab.2019.101038.

Conflicts of interest

The authors have declared no conflict of interest.

References

Badgujar, K.C., Bhanage, B.M., 2016. The green metric evaluation and synthesis of diesel-blend compounds from biomass derived levulinic acid in supercritical carbon dioxide. Biomass Bioenergy 84, 12–21. https://doi.org/10.1016/j.biombioe.2015.11.007.

Badgujar, K.C., Bhanage, B.M., 2014. Application of lipase immobilized on the biocompatible ternary blend polymer matrix for synthesis of citronellyl acetate in non-aqueous media: kinetic modelling study. Enzym. Microb. Technol. 57, 16–25. https://doi.org/10.1016/j.enzmictec.2014.01.006.

Bauer, F., Czihal, S., Bertmer, M., Decker, U., Naumov, S., Wassersleben, S., Enke, D., 2017. Water-based functionalization of mesoporous siliceous materials, Part 1: morphology and stability of grafted 3-aminopropyltriethoxysilane. Microporous Mesoporous Mater. 250, 221–231. https://doi.org/10.1016/j.micromeso.2016.01.046.

Bhange, P., Sridevi, N., Bhange, D.S., Prabhune, A., Ramaswamy, V., 2014. Immobilization of bile salt hydrolase enzyme on mesoporous SBA-15 for co-precipitation of cholesterol. Int. J. Biol. Macromol. 63, 218–224. https://doi.org/10.1016/j.ijbiomac.2013.11.008.

Bhavsar, K.V., Yadav, G.D., 2018. Microwave assisted solvent-free synthesis of n-butyl propionate by immobilized lipase as catalyst. Biocatal. Agric. Biotechnol. 14, 264–269. https://doi.org/10.1016/j.bcab.2018.02.012.

Bommarius, A.S., Paye, M.F., 2013. Stabilizing biocatalysts. Chem. Soc. Rev. 42, 6534. https://doi.org/10.1039/c3cs60137d.

Bradford, M.M., 1976. A rapid and sensitive method for the quantitation of microgram quantities of protein utilizing the principle of protein-dye binding. Anal. Biochem. 72, 248–254. https://doi.org/10.1088/1751-8113/44/8/085201.

Cai, C., Gao, Y., Liu, Y., Zhong, N., Liu, N., 2016. Immobilization of *Candida antarctica* lipase B onto SBA-15 and their application in glycerolysis for diacylglycerols synthesis. Food Chem. 212, 205–212. https://doi.org/10.1016/j.foodchem.2016.05.167.

Calavia, A.P., 2014. Microwave-assisted synthesis of stable SBA-15 mesoporous supports for CaO-based sorbents suitable for CO 2 capture Engenharia Química. https://fenix.tecnico.ulisboa.pt/downloadFile/563345090412708/Dissertacao_Ana%20Pascual.pdf.

Charusheela, A., Arvind, L., 2002. Enzyme catalyzed hydrolysis of esters using reversibly soluble polymer conjugated lipases. Enzym. Microb. Technol. 30, 19–25. https://doi.org/10.1016/S0141-0229(01)00463-X.

Chong, S.M., Zhao, X.S., 2003. Functionalization of SBA-15 with APTES and characterization of functionalized materials. J. Phys. Chem. B 107, 12650–12657. https://doi.org/10.1021/jp035877＋.

Dai, H., Ou, S., Liu, Z., Huang, H., 2017. Pineapple peel carboxymethyl cellulose/polyvinyl alcohol/mesoporous silica SBA-15 hydrogel composites for papain immobilization. Carbohydr. Polym. 169, 504–514. https://doi.org/10.1016/j.carbpol.2017.04.057.

Doadrio, A.L., Sánchez-Montero, J.M., Doadrio, J.C., Salinas, A.J., Vallet-Regí, M., 2014. A molecular model to explain the controlled release from SBA-15 functionalized with APTES. Microporous Mesoporous Mater. 195, 43–49. https://doi.org/10.1016/j.micromeso.2014.04.019.

dos Santos, S.M.L., Nogueira, K.A.B., de Souza Gama, M., Lima, J.D.F., da Silva Júnior, I.J., de Azevedo, D.C.S., 2013. Synthesis and characterization of ordered mesoporous silica (SBA-15 and SBA-16) for adsorption of biomolecules. Microporous Mesoporous Mater. 180, 284–292. https://doi.org/10.1016/j.micromeso.2013.06.043.

El-Nahass, M.N., El-keiy, M.M., Ali, E.M.M., 2018. Immobilization of *horseradish peroxidase* into cubic mesoporous silicate, SBA-16 with high activity and enhanced stability. Int. J. Biol. Macromol. 116, 1304–1309. https://doi.org/10.1016/j.ijbiomac.2018.05.025.

Gao, S., Wang, Y., Diao, X., Luo, G., Dai, Y., 2010. Effect of pore diameter and cross-linking method on the immobilization efficiency of *Candida rugosa* lipase in SBA-15. Bioresour. Technol. 101, 3830–3837. https://doi.org/10.1016/j.biortech.2010.01.023.

González-Delgado, I., Segura, Y., Martín, A., López-Muñoz, M.-J., Morales, G., 2018. *β-Galactosidase* covalent immobilization over large-pore mesoporous silica supports for the production of high galacto-oligosaccharides (GOS). Microporous Mesoporous Mater 257, 51–61. https://doi.org/10.1016/j.micromeso.2017.08.020.

Guzik, U., Hupert-Kocurek, K., Wojcieszyńska, D., 2014. Immobilization as a strategy for improving enzyme properties-Application to oxidoreductases. Molecules 19, 8995–9018. https://doi.org/10.3390/molecules19078995.

He, J., Song, Z., Ma, H., Yang, L., Guo, C., 2006. Formation of a mesoporous bioreactor based on SBA-15 and porcine pancreatic lipase by chemical modification following the uptake of enzymes. J. Mater. Chem. 16, 4307. https://doi.org/10.1039/b606481g.

Holz, J.C.P., Pereira, G.N., Oliveira, J.V., Lerin, L.A., De Oliveira, D., 2018. Enzyme-catalyzed production of emollient cetostearyl stearate using different immobilized commercial lipases under vacuum system. Biocatal. Agric. Biotechnol. 15, 229–234. https://doi.org/10.1016/j.bcab.2018.06.012.

Hu, Y., Tang, S., Jiang, L., Zou, B., Yang, J., Huang, H., 2012. Immobilization of *Burkholderia cepacia* lipase on functionalized ionic liquids modified mesoporous silica SBA-15. Process Biochem. 47, 2291–2299. https://doi.org/10.1016/j.procbio.2012.09.007.

Hude, M.P., Kozinski, J., Dalai, A.K., Yadav, G.D., 2016. Novelty of *penicillium camembertii* lipase supported on glutaraldehyde activated-SBA-15 mesoporous silica for mono-esterification of bioglycerol in non-aqueous media. Int. J. Chem. React. Eng. 14, 919–928. https://doi.org/10.1515/ijcre-2014-0058.

Jaquish, R., Reilly, A.K., Lawson, B.P., Golikova, E., Sulman, A.M., Stein, B.D., Lakina, N.V., Tkachenko, O.P., Sulman, E.M., Matveeva, V.G., Bronstein, L.M., 2018. Immobilized glucose oxidase on magnetic silica and alumina: beyond magnetic separation. Int. J. Biol. Macromol. 120, 896–905. https://doi.org/10.1016/j.ijbiomac.2018.08.097.

Jesionowski, T., Zdarta, J., Krajewska, B., 2014. Enzyme immobilization by adsorption: a review. Adsorption 20, 801–821. https://doi.org/10.1007/s10450-014-9623-y.

Kamble, M.P., Shinde, S.D., Yadav, G.D., 2016. Kinetic resolution of (R,S)-α-tetralol catalyzed by crosslinked *Candida antarctica* lipase B enzyme supported on mesocellular foam: a nanoscale enzyme reactor approach. J. Mol. Catal. B Enzym. 132, 61–66. https://doi.org/10.1016/j.molcatb.2016.06.013.

Kruk, M., Jaroniec, M., Ko, C.H., Ryoo, R., 2000. Characterization of the porous structure of SBA-15. Chem. Mater. 12, 1961–1968. https://doi.org/10.1021/cm000164e.

Li, Y., Zhong, N., Cheong, L.-Z., Huang, J., Chen, H., Lin, S., 2018. Immobilization of *Candida antarctica* Lipase B onto organically-modified SBA-15 for efficient production of soybean-based mono and diacylglycerols. Int. J. Biol. Macromol. 120, 886–895. https://doi.org/10.1016/j.ijbiomac.2018.08.155.

Magadum, D.B., Yadav, G.D., 2017. One-pot synthesis of (R)-1-(pyridin-4-yl)ethyl acetate using tandem catalyst prepared by co-immobilization of palladium and lipase on mesoporous foam: optimization and kinetic modelling. Chirality 29, 811–823. https://onlinelibrary.wiley.com/doi/abs/10.1002/chir.22743.

Magadum, D.B., Yadav, G.D., 2018. Design of tandem catalyst by co-immobilization of metal and enzyme on mesoporous foam for cascaded synthesis of (R)-phenyl ethyl acetate. Biochem. Eng. J. 129, 96–105. https://doi.org/10.1016/j.bej.2017.10.011.

Nakhate, A.V., Yadav, G.D., 2016. Synthesis and characterization of sulfonated carbon-based graphene oxide monolith by solvothermal carbonization for esterification and unsymmetrical ether formation. ACS Sustain. Chem. Eng. 4, 1963–1973. https://doi.org/10.1021/acssuschemeng.5b01205.

Nguyen, T.P.B., Lee, J., Shim, W.G., Moon, H., 2008. Synthesis of functionalized SBA-15 with ordered large pore size and its adsorption properties of BSA. Microporous Mesoporous Mater. 110, 560–569. https://doi.org/10.1016/j.micromeso.2007.06.054.

Poojari, Y., Clarson, S.J., 2013. Thermal stability of *Candida antarctica* lipase B immobilized on macroporous acrylic resin particles in organic media. Biocatal. Agric. Biotechnol. 2, 7–11. https://doi.org/10.1016/j.bcab.2012.10.002.

Rios, N.S., Pinheiro, M.P., dos Santos, J.C.S., de, S., Fonseca, T., Lima, L.D., de Mattos, M.C., Freire, D.M.G., da Silva, I.J., Rodríguez-Aguado, E., Gonçalves, L.R.B., 2016. Strategies of covalent immobilization of a recombinant *Candida antarctica* lipase B on pore-expanded SBA-15 and its application in the kinetic resolution of (R , S)-phenylethyl acetate. J. Mol. Catal. B Enzym. 133, 246–258. https://doi.org/10.1016/j.molcatb.2016.08.009.

Salvi, H.M., Kamble, M.P., Yadav, G.D., 2018. Synthesis of geraniol esters in a continuous-flow packed-bed reactor of immobilized lipase: optimization of process parameters and kinetic modeling. Appl. Biochem. Biotechnol. 184, 630–643. https://doi.org/10.1007/s12010-017-2572-7.

Sheldon, R.A., van Pelt, S., 2013. Enzyme immobilisation in biocatalysis: why, what and how. Chem. Soc. Rev. 42, 6223–6235. https://doi.org/10.1039/C3CS60075K.

Sheldon, R.A., Woodley, J.M., 2018. Role of biocatalysis in sustainable chemistry. Chem. Rev. 118, 801–838. https://doi.org/10.1021/acs.chemrev.7b00203.

Soto, I.D., Escobar, S., Mesa, M., 2017. Study of the physicochemical interactions between *Thermomyces lanuginosus* lipase and silica-based supports and their correlation with the biochemical activity of the biocatalysts. Mater. Sci. Eng. C 79, 525–532. https://doi.org/10.1016/j.msec.2017.05.088.

Yadav, G.D., Borkar, I.V., 2008. Kinetic modeling of immobilized lipase catalysis in synthesis of n-butyl levulinate. Ind. Eng. Chem. Res. 47, 3358–3363. https://doi.org/10.1021/ie800193f.

Yadav, G.D., Jadhav, S.R., 2005. Synthesis of reusable lipases by immobilization on hexagonal mesoporous silica and encapsulation in calcium alginate: transesterification in non-aqueous medium. Microporous Mesoporous Mater 86, 215–222. https://doi.org/10.1016/j.micromeso.2005.07.018.

Yadav, G.D., Trivedi, A.H., 2003. Kinetic modeling of immobilized-lipase catalyzed transesterification of n-octanol with vinyl acetate in non-aqueous media. Enzym. Microb. Technol. 32, 783–789. https://doi.org/10.1016/S0141-0229(03)00064-4.

Yadav, G.D., Yadav, A.R., 2014. Synthesis of ethyl levulinate as fuel additives using heterogeneous solid superacidic catalysts: efficacy and kinetic modeling. Chem. Eng. J. 243, 556–563. https://doi.org/10.1016/j.cej.2014.01.013.

Zdarta, J., Klapiszewski, L., Jedrzak, A., Nowicki, M., Moszynski, D., Jesionowski, T., 2016. Lipase B from *Candida antarctica* immobilized on a silica-lignin matrix as a stable and reusable biocatalytic system. Catalysts 7, 14. https://doi.org/10.3390/catal7010014.

Zdarta, J., Meyer, A., Jesionowski, T., Pinelo, M., 2018a. A general overview of support materials for enzyme immobilization: characteristics, properties, practical utility. Catalysts 8, 92. https://doi.org/10.3390/catal8020092.

Zdarta, J., Meyer, A.S., Jesionowski, T., Pinelo, M., 2018b. Developments in support materials for immobilization of oxidoreductases: a comprehensive review. Adv. Colloid Interface Sci. 258, 1–20. https://doi.org/10.1016/j.cis.2018.07.004.

Zdarta, J., Pinelo, M., Jesionowski, T., Meyer, A.S., 2018c. Upgrading of biomass monosaccharides by immobilized glucose dehydrogenase and xylose dehydrogenase. ChemCatChem 10, 5164–5173. https://doi.org/10.1002/cctc.201801335.

Zhao, D., Huo, Q., Feng, J., Chmelka, B.F., Stucky, G.D., 1998. Nonionic triblock and star diblock copolymer and oligomeric surfactant syntheses of highly ordered, hydrothermally stable, mesoporous silica structures. J. Am. Chem. Soc. 120, 6024–6036. https://doi.org/10.1021/ja974025i.

Zhou, L., He, Y., Ma, L., Jiang, Y., Huang, Z., Yin, L., Gao, J., 2018. Conversion of levulinic acid into alkyl levulinates: using lipase immobilized on meso-molding three-dimensional macroporous organosilica as catalyst. Bioresour. Technol. 247, 568–575. https://doi.org/10.1016/j.biortech.2017.08.134.

Zou, B., Song, C., Xu, X., Xia, J., Huo, S., Cui, F., 2014. Enhancing stabilities of lipase by enzyme aggregate coating immobilized onto ionic liquid modified mesoporous materials. Appl. Surf. Sci. 311, 62–67. https://doi.org/10.1016/j.apsusc.2014.04.210.